

EFFECTS OF CNT ADDED WOVEN CF HEATING ELEMENT ON RESISTANCE WELDING BEHAVIOR OF CF/PPS LAMINATES

Daiki Tanabe¹, Syogo Takahashi¹ and Kazuaki Nishiyabu²

¹ Department of Mechanical Engineering, Kobe City College of Technology,
8-3, Gakuen-Higashimachi, Nishi-ku, Kobe 651-2194, Japan, kcct-tanabe@g.kobe-kosen.ac.jp

² Faculty of Science and Engineering, Kindai University,
3-4-1 Kowakae, Higashiosaka, Osaka 577-8502, Japan, nishiyabu@mech.kindai.ac.jp

Keywords: Resistance welding, CF/PPS, SWCNT, Tensile shear strength, Welding behaviour

ABSTRACT

This study aims to reveal that the effects of carbon nanotube added resistance heating element on resistance welding behavior of woven carbon fiber reinforced polyphenylenesulfide (woven-CF/PPS) laminates. The materials used for resistance welding were woven-CF/PPS laminates and resistance heating element consisting of woven carbon fiber, single-walled carbon nanotube (SWCNT), woven glass fiber and PPS polymer. The stabilized DC power supply for the welding process has a maximum output of 400 W. The push-in amount of pressure jig during welding process were controlled by using an air cylinder device. The effects of SWCNT weight fraction in resistance heating element on resistance welding behavior and actual tensile shear strength were investigated to reveal the welding behavior. The welding part was evaluated by image analysis and microscopic observation. From the experimental results, it was revealed that carbon nanotube weight fraction in the resistance heating element was significantly affects the resistance welding behavior. According to the results of fracture surface observation, it was found that the melting area of welding part was increased by the addition of SWCNT.

1 INTRODUCTION

Carbon fiber reinforced thermoplastic (CFRTP) composites which can be manufactured by press-forming, hybrid injection molding and automated tape laying are attracting attention recently in aircraft and automobile applications[1]. The joining process is a necessary step to manufacture complex geometry parts and large-scaled structures using CFRTP. The joining of thermoplastic composites can be divided into several methods such as mechanical fastening, adhesive bonding and fusion joining or welding [2-4]. The mechanical fastening method has some disadvantages such as stress concentrations, gain of weight and so on. Adhesive bonding method is also difficult to bond chemically between thermoplastic polymers.

Therefore, the fusion joining or welding is suitable for CFRTP parts. There are several types of fusion joining methods for CFRTP such as ultrasonic welding, resistance welding, induction welding and so on, and these heating principles are completely different [5]. The resistance welding method has several advantages such as simple joining device, cost-effective and in applicability to large structures compared to other fusion joining methods[3-6]. Therefore, it was applied to joining between large scaled structures made of CFRTP such as A340 J-nose parts. It has also been widely used for polyethylene pipe systems of gas and water. In those applications, the heating element made of stainless steel mesh and Ni-Cr wire has been used by inserting between joint surfaces [6-10].

Table 1 shows examples of recent research on resistance welding. In this method, resistance heating elements such as stainless steel mesh has been inserted between joint surfaces[7,8,13]. However, the resistance heating elements are undesirable materials which has disadvantage on recyclability, low joining strength and corrosion resistance because the metallic heating elements remains joining parts. Therefore, the materials like carbon fiber are desirable as resistance heating element for resistance welding.

V. Rohart and M. Endrass, including the author, have proposed using carbon fiber as a resistance heating element to solve these problems[11,14]. In our previous study[11], the resistance welding method for CFRTP was developed using spread carbon fiber sheets as resistance heating element. As the result, the single lap tensile shear strength increased at least three times compared to using metallic heating elements, because the fusion layer was reinforced by carbon fiber heating elements. However, in the case of using spread carbon fiber as heating element, the temperature distribution was uneven frequently, because it was difficult to place uniformly the carbon fibers. Therefore, it is not suitable for welding of large scaled structures.

On the other hand, woven carbon fiber is expected to generate stable Joule heating due to the contact resistance at the intersection of fiber bundles and the electrical resistance inside the carbon fiber. In a recent project, resistance welding of UD-CF/LM-PAEK laminates has been demonstrated in A320 MFFD[14]. In order to prevent current leakage from the resistance heating element to the laminate, a resistance heating element insulated with a glass fiber sheet is used.

In recent studies, nanocomposite-based resistance heating elements composed of carbon nanotubes such as MWCNT or CNT-web and thermoplastics have also been proposed to reduce thermal residual stress in fusion joints[15,16]. In order to realize stable temperature distribution and improve bonding strength, it is necessary to investigate the type and amount of carbon nanotubes.

In this study, a woven carbon fiber resistance heating element with SWCNT added was developed to improve the thermal conductivity and bonding strength of the fused part. Specifically, the heating elements were manufactured by melting and kneading single-walled carbon nanotubes and PPS polymer, and the resistance heating element effects on joining strength and melting behavior of welding part were investigated.

Table 1: Comparison of recent resistance welding research for CFRTP

Author	Joining materials	Heating element	Max weld strength
V. Rohart et al. [13]	UD-CF/PPS	Stainless steel mesh with silane coating	37.6 MPa
D. Tanabe et al. [11]	Woven-CF/PPS	Spread-CF/PPS Woven-CF/PPS	30 MPa 24.5 MPa
M. Endrass et al. [14]	UD-CF/LM-PAEK	Woven-CF/LM-PAEK	15795 ± 1089 N
D. Brassard et al. [15]	UD-CF/PEEK	MWCNT/PEI	19.6 MPa
R. Massimiliano et al. [16]	UD-CF/PEKK	CNT-web/PEKK	30 MPa

2 MATERIALS AND EXPERIMENTAL PROCEDURE

2.1 Materials

The materials used for the experiment is CF/PPS laminate (Toray Advanced Composites, CETEX®). This laminate has 5H sateen weave construction with a resin content of $V_f=45\text{vol.}\%$ and a thickness of $t=2.5\text{mm}$ (woven-CF/PPS). The laminate was cut to 60 mm width and 85 mm length using a water jet cutting machine (OMAX, ProtoMAX®) before resistance welding. Plain weave glass fiber (basis weight 30 g/m², thickness $t_{GF}=0.032\text{ mm}$) was used as the insulating layer of the resistance heating element.

The PPS polymer is semi-crystalline polymer. The result of differential scanning calorimeter (DSC) analysis shown that the glass-transition temperature is $T_g=90^\circ\text{C}$, and the melting temperature is $T_m=290^\circ\text{C}$. The result of thermogravimetric analysis (TG) also shown that the decomposition temperature is $T_d=410^\circ\text{C}$.

Plain weave carbon fiber (Toray Co., Ltd., TORAYCA[®], 3K-CF) and PPS film (Toray Co., Ltd., TORELINA[®], thickness $t_{PPS}=0.1\text{mm}$) were used as the resistance heating element. Plain weave glass fiber (basis weight 30 g/m^2 , thickness $t_{GF}=0.032\text{ mm}$) was also used as the insulating layer of the resistance heating element.

In order to manufacture nanocomposites of carbon nanotubes and PPS polymer, single-walled carbon nanotubes (OCSiAl, Tuball[®], 01RW03, outer diameter 1.2-2.0 nm, length $>5\text{ }\mu\text{m}$, SWCNT) shown in Fig. 1(a) and PPS powder (Toray Co., Ltd., TORELINA[®], particle size 100-300 μm) shown in Fig. 1(b) were used.

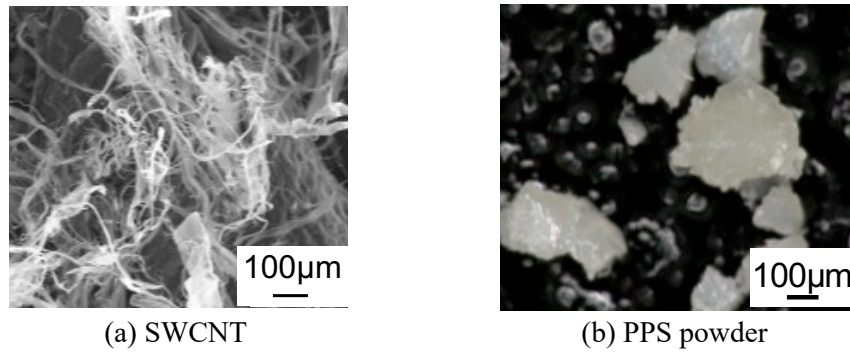


Figure 1: Microscopic images of PPS powder and SWCNT used for SWCNT/PPS nanocomposites.

2.2 Manufacturing method of resistance heating element

Fig.2 shows manufacturing process of SWCNT/PPS nanocomposite sheet. SWCNT have larger fiber lengths and higher thermal and mechanical properties than multi-walled carbon nanotubes (MWCNT), but SWCNT need to be defibrillated due to their strong cohesion. Therefore, the polar solvent N-methyl-2-pyrrolidone (NMP) was used to defibrillate SWCNT using ultrasonic vibration. These materials were compounded by heat kneading at mold temperature of 310°C . Subsequently, the nanocomposites was molded into sheets 0.1mm thick by vacuum hot press molding machine. After that, the SWCNT/PPS sheet was cut into 23 mm width and 120 mm length using an ultrasonic cutter.

Fig.3 shows the stacking sequence of the resistance heating element. PPS polymer and SWCNT/PPS were impregnated into plain weave carbon fiber and plain weave glass fiber. The impregnated sheets were laminated into any stacking sequence and integrated using the vacuum hot press device.

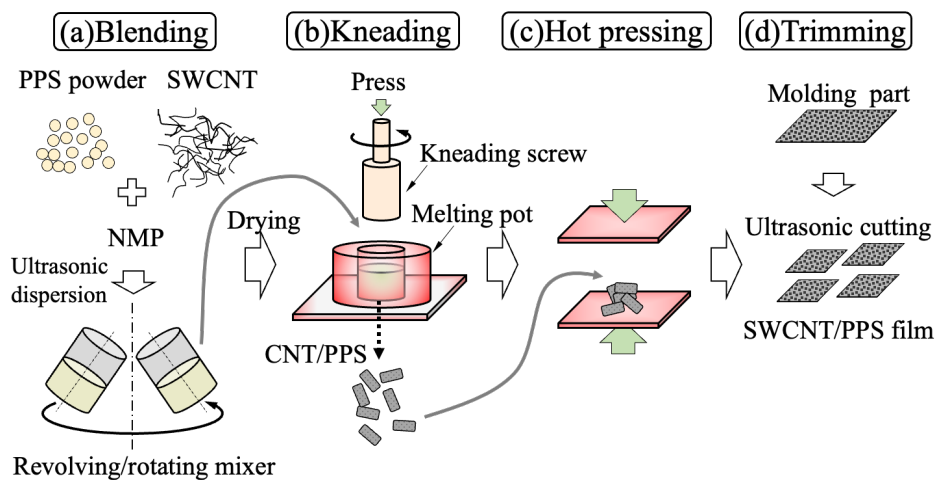


Figure 2: Manufacturing process of SWCNT/PPS nanocomposites.

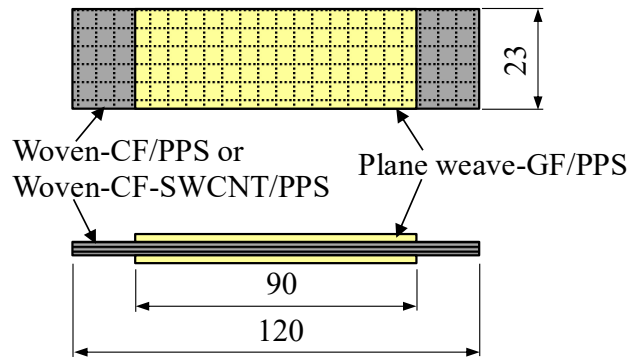


Figure 3: Stacking sequence of resistance heating element.

2.3 Resistance welding method

Fig.4 shows the schematic drawing of resistance welding device. The woven-CF/PPS laminates with $W=60\text{mm}$ in width and $L=85\text{mm}$ in length were prepared. The welding area is insofar as $L_f=20\text{mm}$ from the end of laminates.

The test specimen was clipped by insulating plates made of ceramics and the applied current controlled by a stabilized DC power supply (Kikusui Electronics Co., Ltd., PBZ20-20) was applied to resistance heating element. This made generate a joule heat in the joint interface between laminates, thus made melt the PPS polymer. To prevent a current leakage between the test specimen and electrode, Kapton® polyimide film (Du Pont-Toray Co., Ltd., Type H, 0.05mm in thickness) which possesses high heat resistance and electrical resistance was inserted as shown in Fig 4.

Moreover, the welding load was measured by load cells during the resistance welding. The resistance welding process mainly consists of 4 steps; (a) Fixation of the test specimens to welding device, (b) Application of applied load ($P=1\text{ kN}$) with pressing machine, (d) Applied current to generate joule heat in holding several time ($t=180\text{s}$), and (e) Turning off the electric voltage and cooling of the matrix polymer for solidification.

The resistance heating element was mounted between laminates to work as the heating element. The test specimen was clipped by insulating plates made of ceramics and the applied voltage ($E=20\text{V}$ const.) controlled by a stabilized DC power supply was applied to resistance heating element. This made generate a joule heat in the joint interface between laminates, thus made melt the PPS polymer.

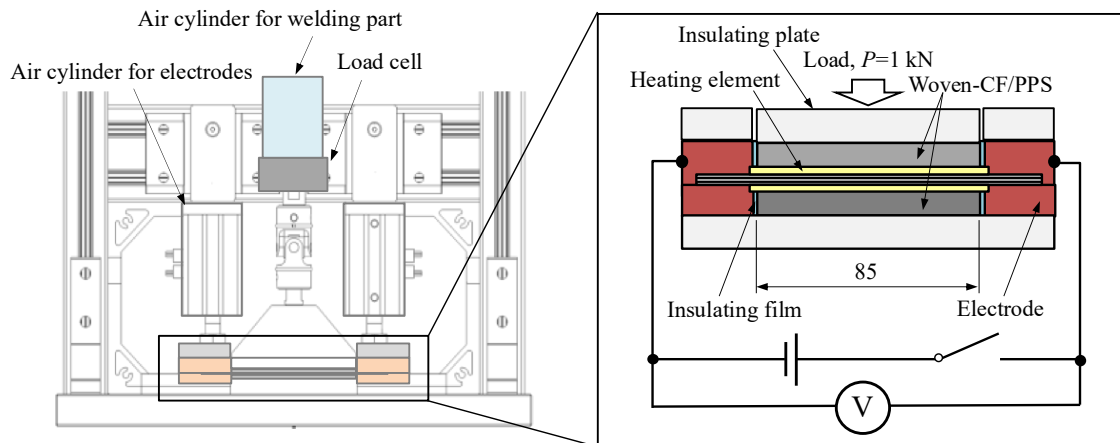


Figure 4: Appearance of resistance welding device.

2.4 Evaluation method

In order to evaluate the morphology of SWCNT inside the SWCNT/PPS nanocomposites, microscopic observation was performed using a scanning electron microscope (JEOL Ltd., JSM-IT200). To quantitatively evaluate the dispersion of SWCNT inside the SWCNT/PPS nanocomposites, the volume resistivity ρ_v [$\Omega \cdot \text{cm}$] was also measured using a four-point probe method with a resistivity meter (Nittoseiko Analytech Co., Ltd., Loresta AX, MCP-T370).

The welding temperature between the resistance heating element and the laminate was measured by using ultra fine K-type thermocouples with 0.076 mm diameter to investigate the resistance welding behavior as shown in Fig.5. During the resistance welding, the applied load and displacement of the joint were measured by a servo press.

The joint surfaces peeled off after joining were recorded with a scanner device, and the welding area (A_w) was measured by image analysis (Image J). Fig.6 shows appearance of single lap tensile shear test specimen. The welded specimens were cut into 20 mm wide specimen using a wet cutting machine. Before single lap tensile shear test, aluminum tabs were bonded to end of specimens with epoxy adhesive. The single lap tensile shear strength test was carried out to evaluate a joint strength by using universal testing machine (SHIMADZU Co., Ltd., AG-Xplus 100kN). The cross-head speed was $v=1\text{mm/min}$. The tensile shear strength was calculated by using this equation:

$$\tau = \frac{P_{max}}{A} \quad (1)$$

where τ , lap shear strength [MPa]; A_w , A , overlap area [mm] and P , maximum tensile force [N].

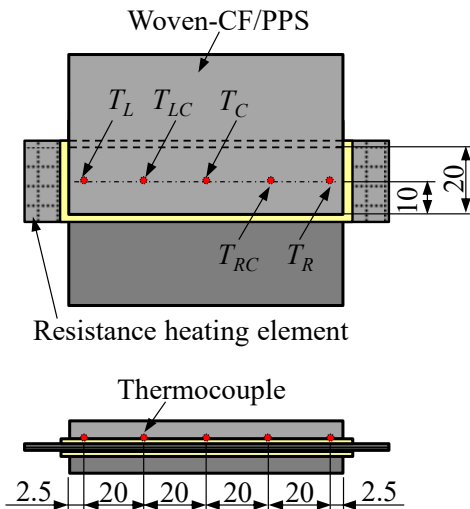


Figure 5: Stacking sequence of resistance heating element.

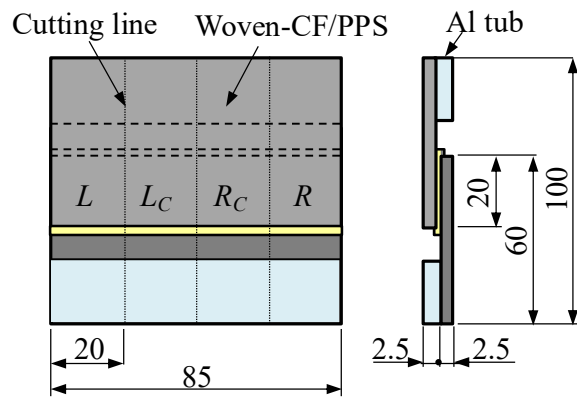


Figure 6: Schematic drawing of single lap shear strength.

3 EXPERIMENTAL RESULTS AND DISCUSSIONS

3.1 Fabrication results of SWCNT/PPS resistance heating element and electrical/thermal characteristics

Fig. 7 shows SEM images of SWCNT/PPS nanocomposites with 0.1wt%, 0.5wt% and 1.0wt% addition of SWCNT to PPS polymer. When 0.1wt% and 0.5wt% of SWCNTs were added to PPS polymer, it was found that SWCNT dispersed uniformly in PPS polymer. It was also found that the SWCNT were entangled with each other to form a three-dimensional network structure in the PPS polymer. The three-dimensional network structure of SWCNT may affect the heat generation properties

and thermal conductivity during resistance welding. On the other hand, when 1 wt% of SWCNT was added to PPS polymer, it was found that SWCNT aggregated. A higher addition rate of SWCNT improves electrical and thermal conductivity, but it is thought that this may lead to a decrease in joining strength.

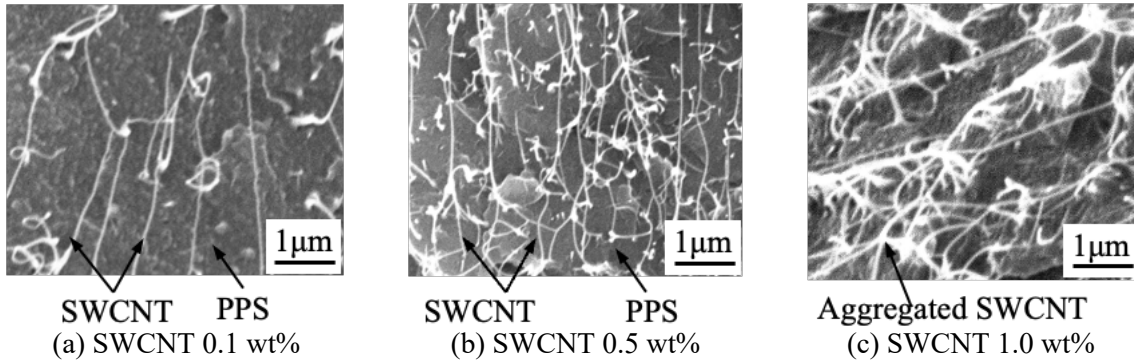


Figure 7: SEM images of SWCNT/PPS nanocomposites.

Fig.8 shows the effects of SWCNT weight fraction on volume resistivity obtained by four-terminal resistance measurement method. When the amount added was less than 0.5 wt%, the volume resistivity showed a relatively high value. It was also found that the volume resistivity decreased remarkably when SWCNT was added to 1 wt% or more. Since SWCNT has a high aspect ratio, it was thought that adding 1.0 wt% increases the volume fraction in PPS polymer. This result indicates that a percolation threshold exists at about 1 wt% addition.

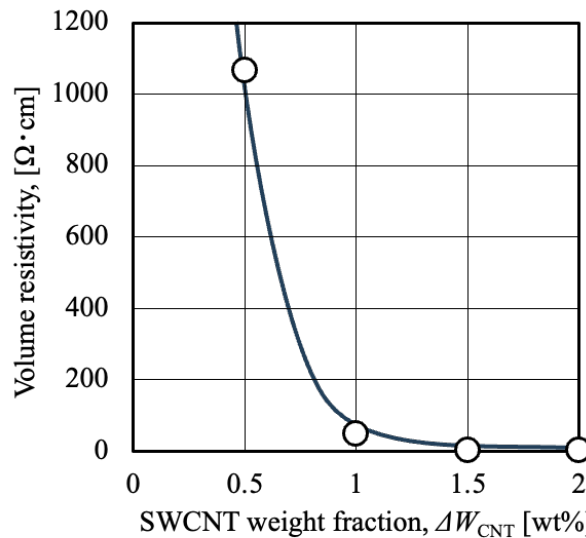


Figure 8: Effects of SWCNT weight fraction on volume resistivity.

Fig.9 shows temperature distribution images of various resistance heating elements obtained by infrared thermography. These thermal images were the results of electric heating by applying current of 3A for 180 s. As a general trend, a temperature drop was observed at both ends of the resistance heating element. The reason for this is thought to be that the resistance heating element is in contact with the copper electrode and dissipates heat. It was found that the temperature distribution of the resistive heating element to which 1 wt% of SWCNT was added became uneven locally. This is considered to be due to aggregation of SWCNT. Moreover, when the SWCNT content increased, the melt viscosity of the PPS polymer increased, which may cause poor contact between the carbon fiber fabric inside the resistance heating element and the SWCNT. However, during resistance welding, the contact resistance is thought to decrease due to the forced compressive load, which may lead to different heating behavior.

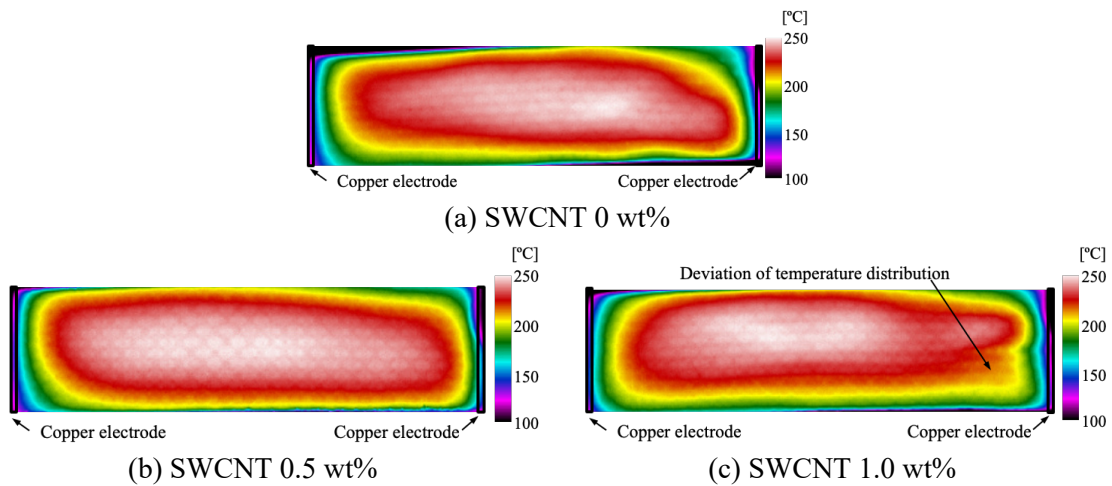


Figure 9: Temperature distribution images of various resistance heating elements obtained by infrared thermography.

3.2 Process monitoring results during resistance welding

Fig.10 shows the result of process monitoring of welding part temperature and welding load during the resistance welding process. The temperature of the welded part was measured at the center of the specimen (T_c). The overall trend was that the electric conducting time was increased with increasing the welding part temperature. Moreover, it was found that the load on the welding part was increased immediately after the start of welding. It was also revealed that above the melting temperature of PPS polymer, the load was decreased significantly.

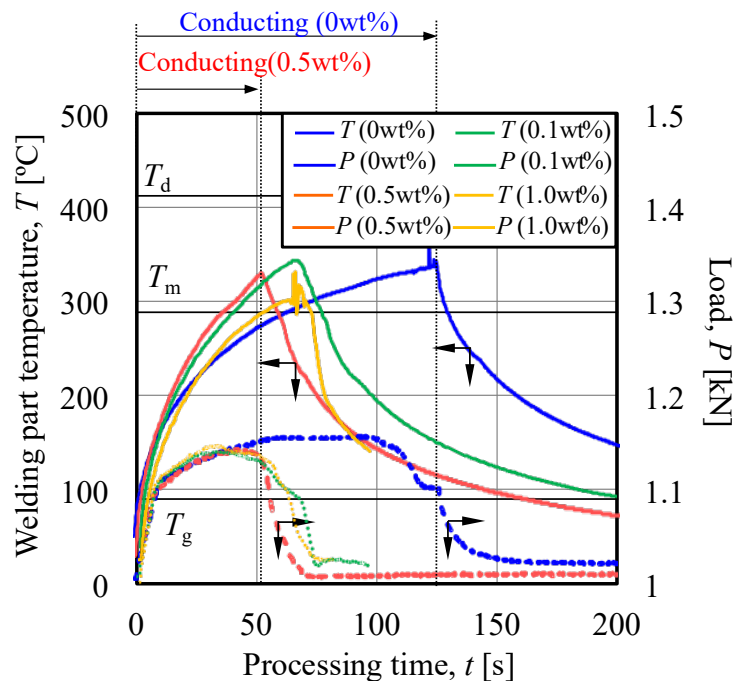


Figure 10: The result of process monitoring during the resistance welding process at various SWCNT weight content.

In the case of SWCNT 0 wt%, it was found that it took 150s to melting of PPS. However, the temperature was below the melting temperature of PPS polymer. In the case of SWCNT 0.5 wt%, the temperature was reached above the melting point in around 50 seconds. This result indicated that the temperature increase rate was faster than that without the addition of SWCNTs. It was considered that the noise above melting temperature of PPS due to outflow of PPS and current leakage to the thermocouples.

Fig.11 shows the effects of SWCNT weight fraction on time to reach melting temperature of PPS polymer. It was found that when the SWCNT weight content was 0 wt% or 0.1 wt%, there was a difference in the heating rate between the center (*C*) and edge (*L*, *R*) of the welded part. This is thought to be due to the heat dissipation on the copper electrodes side, which has high thermal conductivity. It was also found that adding 0.5wt% of SWCNT decreased the difference in heating rate between the center and the edge. From these experimental facts, it was found that the addition of SWCNTs increased the heating area and thermal conductivity of the resistance heating element, and shortened the welding time.

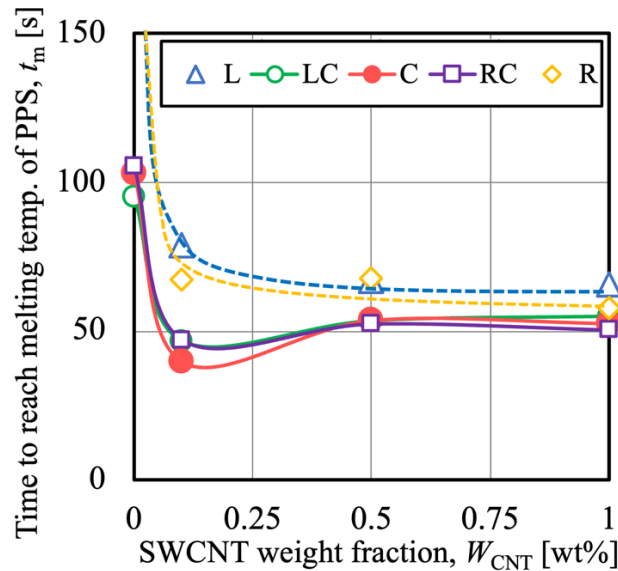


Figure 11: Effects of SWCNT weight fraction on time to reach melting temperature of PPS polymer.

3.3 Effects of addition of SWCNT on resistance welding behavior

Fig.12 shows the scan images of welding surface with 0 wt%, 0.1 wt% and 0.5 wt% SWCNTs. These specimens were observed by using the microscope after tensile shear strength test. In the case of SWCNT 0wt%, the un-melted area of PPS polymer were observed at the edge of welding part. This is because the heat dissipation was occurred to the copper electrode.

The welding area was increased with increasing the weight fraction of SWCNT to PPS polymer. In the case of SWCNT 0 wt% and 0.1 wt% specimens, the fracture of the glass fiber was observed significantly. On the other hand, in the case of SWCNT 0.5 wt%, the fracture of carbon fiber bundles of laminates was occurred because the melting of PPS polymer was performed significantly.

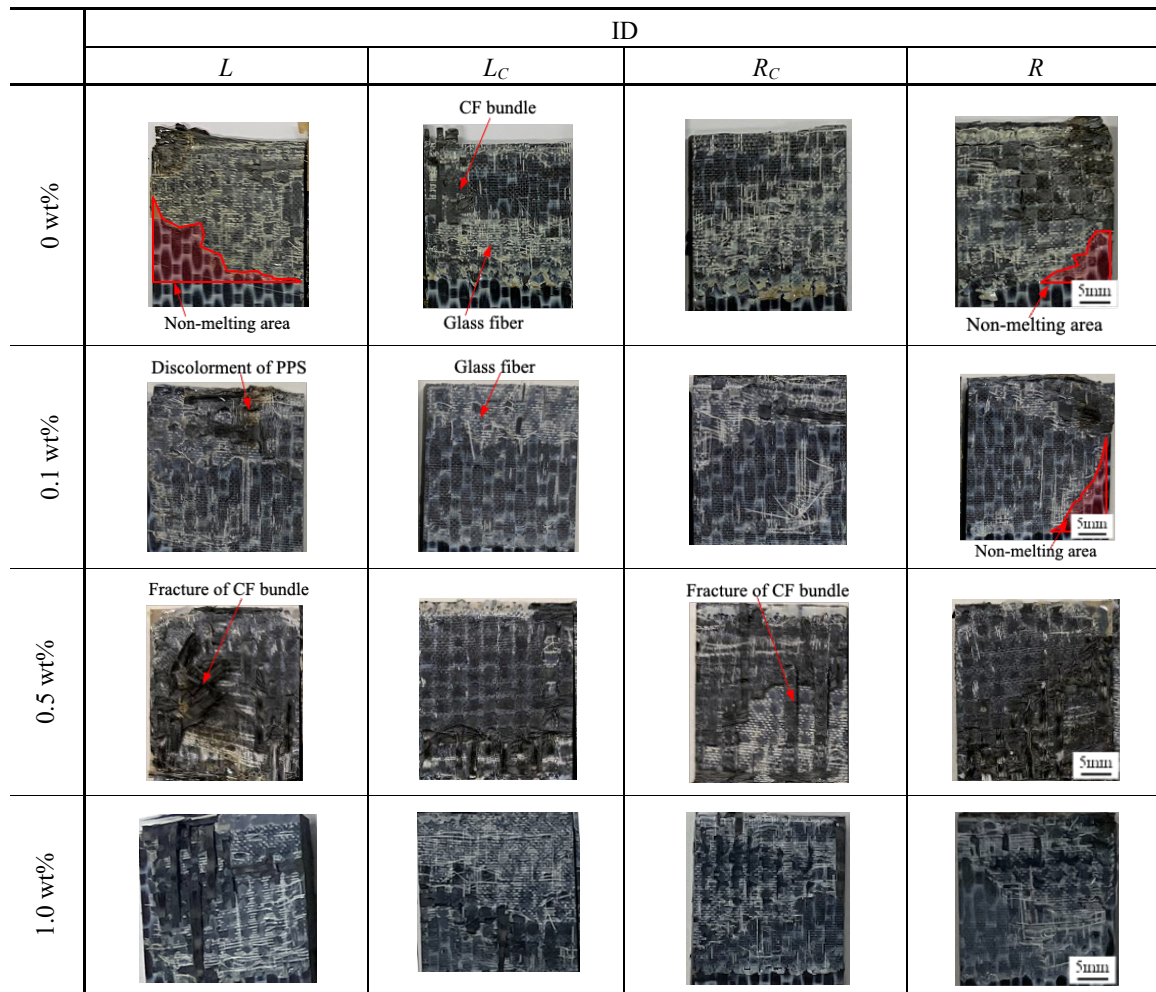


Figure 12: Scan images of peeled face with 0 wt%, 0.1 wt%, 0.5 wt% and 1.0 wt% SWCNTs.

3.4 Effects of addition of SWCNT on tensile shear strength

Fig.13 shows P - δ curve obtained by tensile shear strength at various SWCNT content. It was found that the addition of SWCNT increased the fracture strain. This result suggests that the addition of SWCNT improves the toughness of the welded part. In the case of specimen with 0.5wt% SWCNT added, the maximum load was increased significantly because SWCNT were uniformly dispersed in the PPS polymer and formed a three-dimensional nano-network structure. In the case of specimen with 1.0wt% SWCNT added, it was considered that the volume fraction of SWCNTs was high and aggregation of SWCNT occurred, and the maximum load did not improve.

Fig.14 shows the effects of SWCNT weight fraction of resistance heating element on tensile shear strength. The tensile shear strength was increased with increasing the SWCNT weight fraction. The tensile shear strength at the edge of the joint was lower than that at the center of the joint. The addition of SWCNT to the resistance heating element was increased the Joule heating value and thermal conductivity, and promoted the melting of the PPS polymer. The effectiveness of adding SWCNT to resistance heating elements was revealed from the results of these experiments.

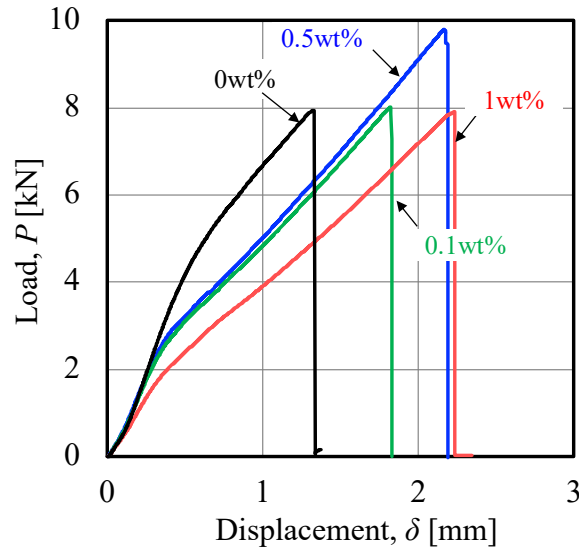


Figure 13: P - δ curve obtained by tensile shear test.

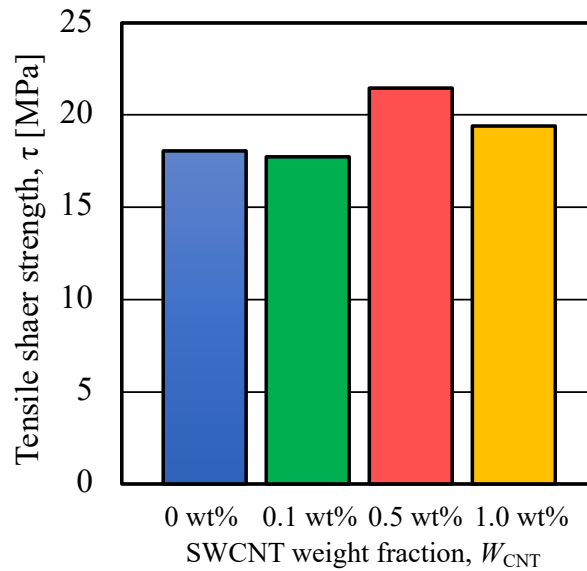


Figure 14: Effects of SWCNT weight fraction of resistance heating element on tensile shear strength.

Fig.15 shows SEM images of fracture face at various SWCNT weight fraction. In the case of specimen with 0 wt% SWCNT, the fracture of the glass fiber was observed significantly. Therefore, it was suggested that the interfacial strength between glass fiber and PPS polymer should be improved. In the case of specimen with 0.5 wt% SWCNT added, fiber breakage occurred in the woven carbon fiber inside the resistance heating element. It was also found that SWCNT were isolated and dispersed around the carbon fibers. It was considered that the bonding strength was improved because SWCNT reinforced the carbon fiber inside the resistance heating element and the surroundings of the PPS resin with nanofibers. In the case of specimen with 1.0 wt% SWCNT added, it was observed that the SWCNTs were entangled and aggregated. Therefore, it was thought that the decrease in strength occurred at locations where SWCNTs were locally aggregated.

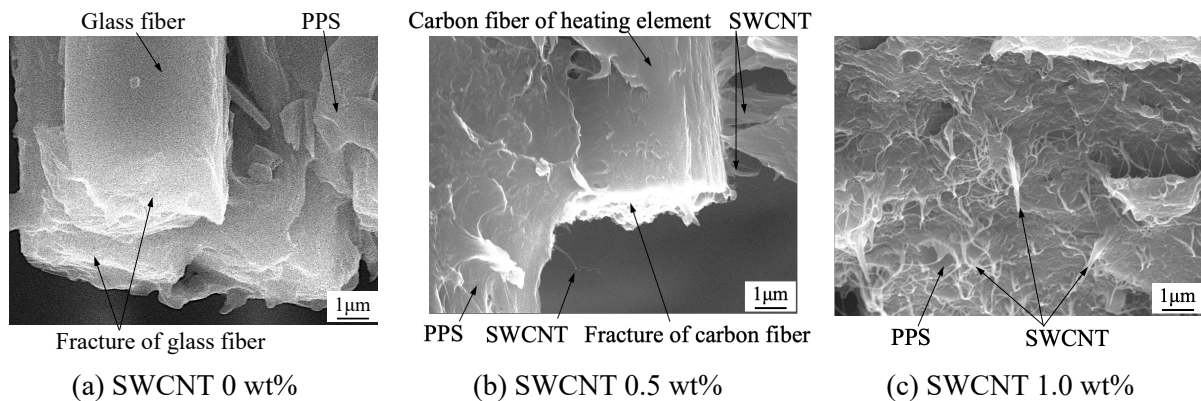


Figure 15: SEM images of fracture face at various SWCNT weight fraction.

4 CONCLUSIONS

This study aims to reveal that the effects of carbon nanotube added resistance heating element on resistance welding behavior of woven carbon fiber reinforced polyphenylenesulfide (woven-CF/PPS) laminates. The effects of SWCNT weight fraction in resistance heating element on resistance welding behavior and actual tensile shear strength were investigated to reveal the welding behavior.

From the experimental results, it was revealed that carbon nanotube weight fraction in the resistance heating element significantly affects the resistance welding behavior and tensile shear strength. According to the results of fracture surface observation, it was found that the melting area of welding part was increased by the addition of SWCNT. The effectiveness of adding SWCNT to resistance heating elements was revealed from the results of these experiments.

REFERENCES

- [1] M. Yamane, "Technologies of Carbon Fiber Reinforced Thermoplastics -Material · Molding · Recycle-", *Science&Technology Co.,Ltd.*, (2015).
- [2] A. Yousefpour, M. Hojjati and J. Immarigeon, "Fusion Bonding/Welding of Thermoplastic Composites", *Journal of Thermoplastic Composite Materials*, Vol.17. (2004),
- [3] A. Köver et al., "Simulation and Manufacturing of an Automotive Part for Mass Production", *Proceedings of 2nd International Conference and Exhibition on Thermoplastic Composites (ITHEC2014)*, A-3, (2014), pp.21-25.
- [4] C. Callens and F. Bordellier, "QSP®: How to Produce a Netshape Thermoplastic Composite Part in One Minute", *Proceedings of 3rd International Conference and Exhibition on Thermoplastic Composites (ITHEC2016)*, A-3, (2016), pp.24-27.
- [5] I.F. Villegas, L. Moser, A. Yousefpour, P. Mitschang and H.E. Bersee, "Process and performance evaluation of ultrasonic, induction and resistance welding of advanced thermoplastic composites", *Journal of Thermoplastic Composite Materials*, Vol.28, No.8 (2012), pp.1007-1024.
- [6] T.J.Ahmed, D. Stavrov, H.E.N. Bersee and A. Beukers, "Induction welding of thermoplastic composites—an overview", *Composites: Part A*, 37 (2006), pp.1638-1651.
- [7] M. Dube', P. Hubert, A. Yousefpour and J. Denault, "Resistance welding of thermoplastic composites skin / stringer joints", *Composites: Part A*, 38 (2007), pp.2541-2552.
- [8] D. Stavrov and H.E.N. Bersee, "Resistance welding of thermoplastic composites-an overview", *Composites: Part A*, 36 (2005), pp.39-54.

- [9] D. Tanabe, K. Nishiyabu and T. Kurashiki, “Effects of fiber reinforcing configuration on oxidation and melting phenomenon of CF/PPS laminated composites by electrically-conducting”, *Journal of The Society of Materials Science*, Vol.63 No.5 (2014a), pp.368-373.
- [10] D. Tanabe, K. Nishiyabu and T. Kurashiki, “Electro-fusion behavior of CF/PPS laminates using Ni-Cr wire resistance heating element”, *Transactions of the JSME (in Japanese)*, Vol.80, No.815 (2014b), DOI: 10.1299/transjsme.2014smm0189.
- [11] D. Tanabe, K. Nishiyabu and T. Kurashiki, “Effects of processing parameters on electro-fusion joining of CF/PPS composites using carbon fiber heating elements”, *Transactions of the JSME*, Vol.81, No.826 (2015), DOI: 10.1299/transjsme.15-00005.
- [12] D.Tanabe, F. Kubohori, K. Tamura and K. Nishiyabu, “Effects of Dimension of Joining Part on Welding Behavior of Carbon Fiber Reinforced Thermoplastics using Spread and Woven Carbon Fiber Resistance Heating Element”, *Journal of the Society of Materials Science, Japan*, Vol.68, No. 2 (2019), DOI; doi.org/10.2472/jsms.68.162.
- [13] V. Rohart, L.L. Lebel and M. Dubé, “Improved adhesion between stainless steel heating element and PPS polymer in resistance welding of thermoplastic composites”, *Composites Part B*, vol.188, (2020), pp.107806.
- [14] M. Endrass et al., “Resistance welding of low-melt polyallyl ether ketone: Process Definition and Optimization”, *Proceedings of the 20th European Conference on Composite Materials*, “(2022).
- [15] D. Brassard, M. Dubé and J. R. Tavares, “Resistance welding of thermoplastic composites with a nanocomposite heating element”, *Composites Part B*, vol.165 (2019), pp.779–784.
- [16] R. Massimiliano, C. Giuseppe, H. Stephen and F.Brian, “Resistance welding of carbon fibre reinforced PEKK by means of CNT webs”, *Journal of Composite Materials*, vol.57, No.1 (2022).